Collector optimization for tradeoff between breakdown voltage and cut-off frequency in SiGe HBT*

Fu Qiang(付 强)[a)b)†], Zhang Wan-Rong(张万荣)[a)], Jin Dong-Yue(金冬月)[a)], Ding Chun-Bao(丁春宝)[a)], Zhao Yan-Xiao(赵彦晓)[a)], and Lu Dong(鲁 东)[a)]

[a)] *College of Electronic Information and Control Engineering, Beijing University of Technology, Beijing* 100124, *China*
[b)] *College of Physics, Liaoning University, Shenyang* 110036, *China*

(Received 22 October 2013; revised manuscript received 8 April 2014; published online 10 September 2014)

As is well known, there exists a tradeoff between the breakdown voltage BV_{CEO} and the cut-off frequency f_T for a standard heterojunction bipolar transistor (HBT). In this paper, this tradeoff is alleviated by collector doping engineering in the SiGe HBT by utilizing a novel composite of P^+ and N^- doping layers inside the collector–base (CB) space-charge region (SCR). Compared with the single N-type collector, the introduction of the thin P^+ layers provides a reverse electric field weakening the electric field near the CB metallurgical junction without changing the field direction, and the thin N^- layer further effectively lowers the electric field near the CB metallurgical junction. As a result, the electron temperature near the CB metallurgical junction is lowered, consequently suppressing the impact ionization, thus BV_{CEO} is improved with a slight degradation in f_T. The results show that the product of $f_T \times BV_{CEO}$ is improved from 309.51 GHz·V to 326.35 GHz·V.

Keywords: SiGe heterojunction bipolar transistors (HBTs), breakdown voltage, cut-off frequency, collector optimization

PACS: 44.10.+i, 72.20.Pa, 85.30.De **DOI:** 10.1088/1674-1056/23/11/114402

1. Introduction

SiGe heterojunction bipolar transistors (HBTs) have emerged as a strong contender in various millimeter-wave and radio-frequency (RF) applications, which is ascribed to the rapid increase in cut-off frequency over recent years.[1–3] The cut-off frequency f_T can be improved by increasing the collector doping concentration, which is mainly due to a reduction in the base–collector space-charge layer width, decreasing the collector–base (CB) transit time (τ_{CSCL}). However, it inevitably results in a decrease of the breakdown voltage (e.g., base-opened collector–emitter breakdown voltage BV_{CEO}) due to the enhanced impact ionization, which certainly affects SiGe HBT competitiveness in millimeter-wave and radio-frequency power applications with respect to III–V HBTs.[4] Therefore, the simultaneous optimization of both f_T and BV_{CEO} in a given technology is challenging due to the process limitations set by the requirements of the high speed device. Currently, device engineers mostly devote their efforts to improving BV_{CEO} at the expense of f_T.[5–10] In this paper, a novel composite of P^+ and N^- doping layers deep in the CB space-charge region (SCR) readjusts the electric field near the CB metallurgical junction to lower the electron temperature, consequently suppressing the impact ionization, which improves BV_{CEO} with little degradation in f_T, and thus improves the well-known tradeoff between the breakdown voltage and the cut-off frequency in the SiGe HBT.

2. Simulation and calculation

TCAD SILVACO software is used to perform the two-dimensional (2D) device simulations. Advanced parameter models are applied to accurately simulate the effects of the avalanche behavior in the SiGe HBT, such as the temperature and concentration dependent carrier mobility model (ARORA), parallel electrical field dependent model (FLDMOB), doping-induced bandgap narrowing model (BGN), temperature and concentration dependent carrier generation-recombination model (HNSAUG), and temperature dependent models (SELB). The carrier temperature equation for the dominant carriers is solved together with the electrostatic Poisson equation and the carrier continuity equations used in the BlOCK and NEWTON iteration methods. Figure 1 shows the cross-section of the SiGe HBT used in SILVACO/ATHENA, and the doping profile for a standard SiGe HBT is shown in Fig. 2.

In order to accurately model the avalanche behavior in an SiGe HBT, the ionization coefficient is calculated via the Okuto–Crowell model with the driving force derived from the electron temperature T_n, which is regarded as an indication of the electron kinetic energy. The electron ionization coefficient α_n can be expressed as[11]

$$\alpha_n(E_n^{\text{eff}}) = a(1 + c(T_n - T_0))E_n^{\text{eff}}$$

*Project supported by the National Natural Science Foundation of China (Grant Nos. 60776051, 61006059, and 61006044), the Beijing Municipal Natural Science Foundation, China (Grant Nos. 4142007, 4143059, 4082007, and 4122014), and the Beijing Municipal Education Committee, China (Grant Nos. KM200710005015 and KM200910005001).

†Corresponding author. E-mail: duduffqq@sohu.com

© 2014 Chinese Physical Society and IOP Publishing Ltd

$$\times \exp\left(\frac{b[1+d(T_n-T_0)]}{E_n^{\text{eff}}}\right)^{\delta}, \qquad (1)$$

where a, b, c, and d are fitting parameters. The electron needs to travel a longer distance in the electric field to gain enough kinetic energy to produce the impact ionization. The electron kinetic energy is mainly obtained near the CB metallurgical junction, where the higher electric field rapidly accelerates the electron.[12] Therefore, the decrease of the electric field near the CB metallurgical junction can lower the electron kinetic energy and lower the electron temperature, consequently suppressing the impact ionization and eventually improving BV_{CEO}.

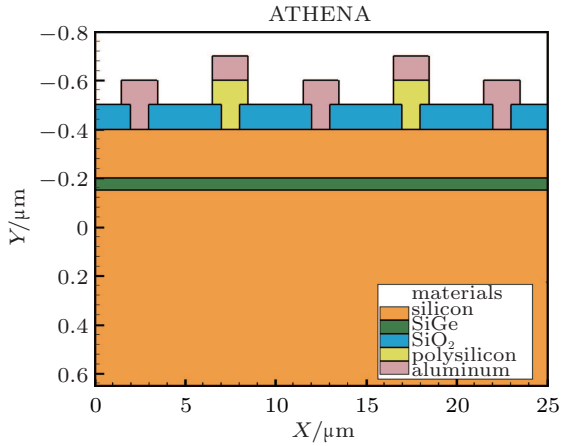


Fig. 1. (color online) Cross-section of SiGe HBT used in SILVACO/ATHENA.

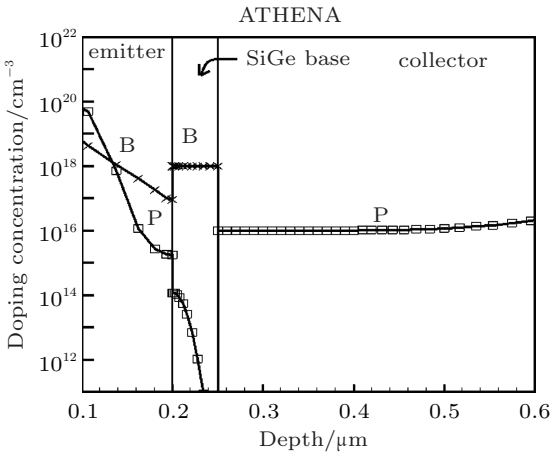


Fig. 2. Doping profile of a standard SiGe HBT used in SILVACO/ATHENA.

3. Result and discussion

For a standard SiGe HBT, the improvement of BV_{CEO} can be obtained by decreasing the collector doping concentration, as shown in Fig. 3. BV_{CEO} improves from 3.7 V to 5.7 V. However, it inevitably widens the CB SCR, giving rise to a higher CB transit time (τ_{CSCL}), and therefore degrading f_T (see Fig. 4). The peak f_T decreases from 70.6 GHz to 54.3 GHz.

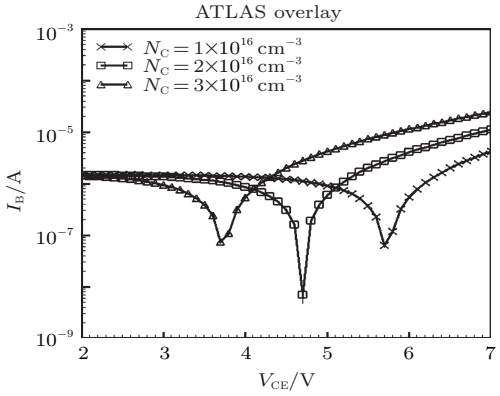


Fig. 3. Absolute value of the base current versus V_{CE} for standard HBTs with different collector doping concentrations.

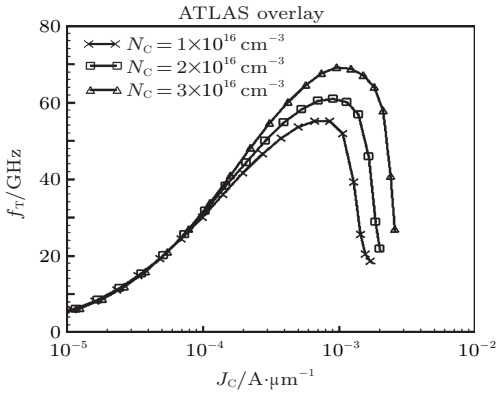


Fig. 4. Comparison of f_T versus J_C for standard HBTs with different collector doping concentrations.

The improvement of BV_{CEO} is ascribed to the lowered electric field near the CB metallurgical junction as the collector doping concentration decreases (see Fig. 5), and it also means that the kinetic energy of the electrons that get accelerated to near the CB metallurgical junction is decreased correspondingly.[13,14] As a result, the peak T_n near the CB metallurgical junction is lowered accordingly (see Fig. 6). Due to the exponential dependence of α_n on T_n, α_n near the CB metallurgical junction is lowered significantly, as shown in Fig. 7. Meanwhile, the lowered electric field near the CB metallurgical junction causes a part of the higher electric field to be somehow shifted deeper into the CB SCR, which does not increase T_n and α_n near the CB metallurgical junction.[15]

To readjust the shape of the electric field, a novel way of improving BV_{CEO} is to use a composite of P^+ and N^- doping layers inside the CB SCR. In addition to the collector doping, all other doping profiles of the devices are kept the same so that an unambiguous comparison can be made. Two novel collector dopings called ColA and ColB are presented, as shown in Fig. 8, which are obtained respectively by only introduction of P^+ (2×10^{16} cm^{-3}) doping layers and inserting a composite of P^+ (2×10^{16} cm^{-3}) and N^- (8×10^{15} cm^{-3}) doping layers inside the CB SCR for a standard SiGe HBT with the single collector doping of $N_C = 1\times10^{16}$ cm^{-3}. Figure 9 shows the absolute value of the base current as a function

of V_{CE} for HBTs with a standard ($N_C = 1 \times 10^{16}$ cm^{-3}) collector doping, ColA, and ColB. Compared with the standard ($N_C = 1 \times 10^{16}$ cm^{-3}) collector doping, BV_{CEO} with ColA is improved by 0.1 V, only a 1.8% increase, while BV_{CEO} with ColB is improved by 0.4 V, a 7% increase, which is a magnitude of clear importance to circuit designers.

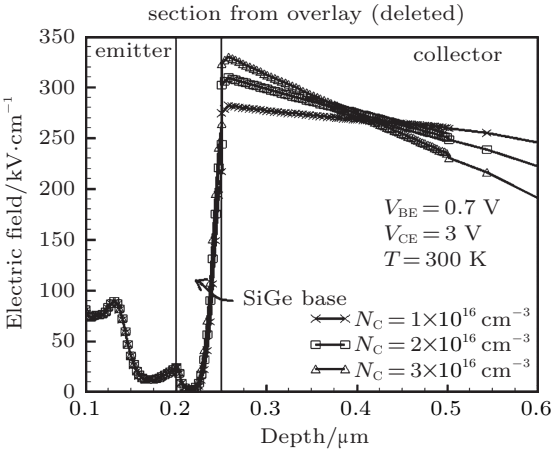


Fig. 5. Comparison of electric field for standard HBTs with different collector doping concentrations.

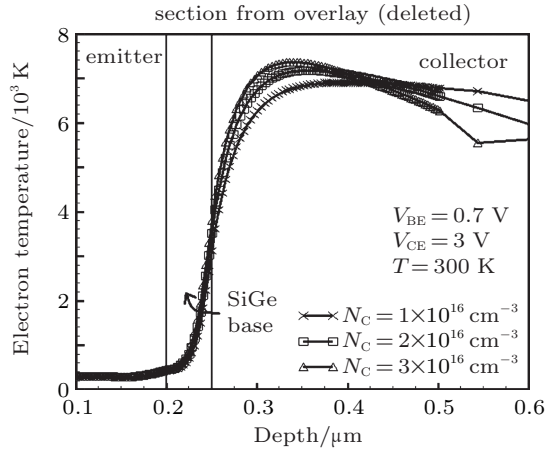


Fig. 6. Comparison of electron temperature for standard HBTs with different collector doping concentrations.

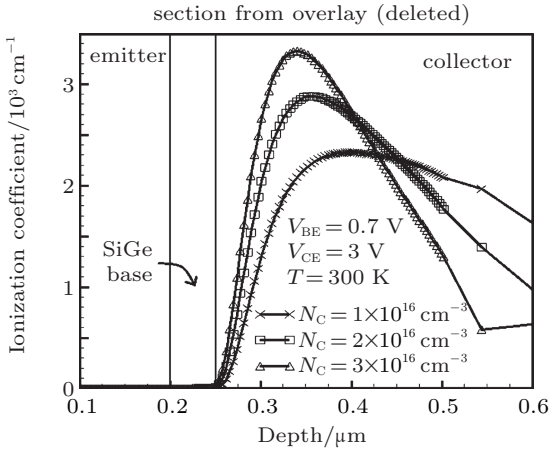


Fig. 7. Comparison of ionization coefficient for standard HBTs with different collector doping concentrations.

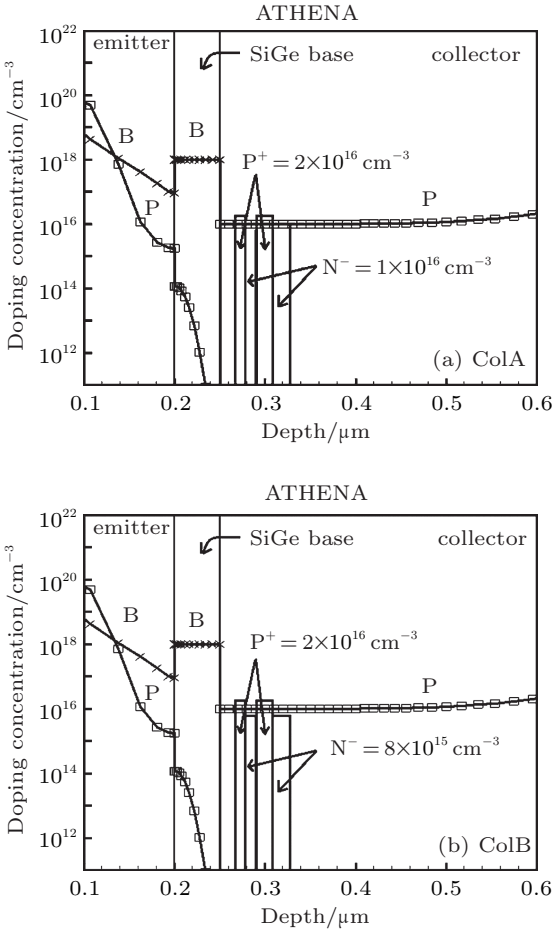


Fig. 8. Doping profiles of HBTs used in SILVACO/ATHENA including a standard ($N_C = 1 \times 10^{16}$ cm^{-3}) collector doping and two novel collector dopings called (a) ColA and(b) ColB.

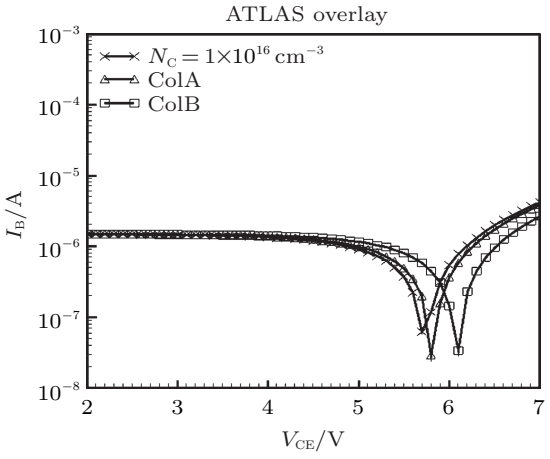


Fig. 9. Absolute value of the base current versus V_{CE} for HBTs with a standard ($N_C = 1 \times 10^{16}$ cm^{-3}) collector doping, ColA, and ColB.

Figure 10 shows the comparison of electric field for HBTs with a standard ($N_C = 1 \times 10^{16}$ cm^{-3}) collector doping, ColA, and ColB. Compared with the standard collector doping, the thin P^+ layer of ColA can provide a reverse electric field weakening the electric field near the CB metallurgical junction without changing the field direction, and the additional thin N^- layer of ColB can further decrease the electric field near the CB metallurgical junction. Furthermore, the P^+ and

N^- doping layers inside the CB SCR cause the higher electric field to shift deeper into the CB SCR. As a result, the electric field near the CB metallurgical junction with ColB is the lowest, and the electric field near the CB metallurgical junction with the standard collector doping is the highest. Therefore, T_n and α_n near the CB metallurgical junction with ColB are the lowest, and T_n and α_n near the CB metallurgical junction with the standard collector doping are the highest, as shown in Figs. 11 and 12.

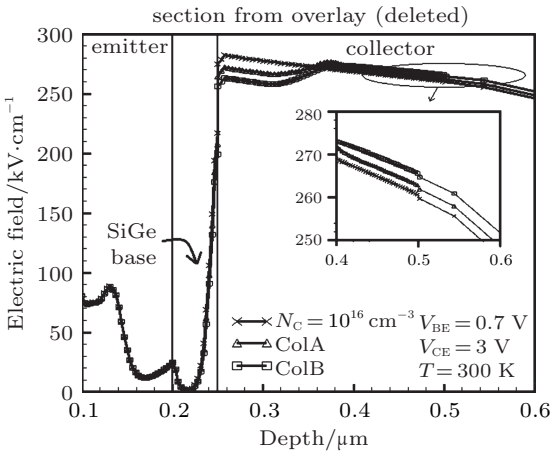


Fig. 10. Comparison of electric field for HBTs with a standard ($N_C = 1 \times 10^{16}$ cm^{-3}) collector doping, ColA, and ColB.

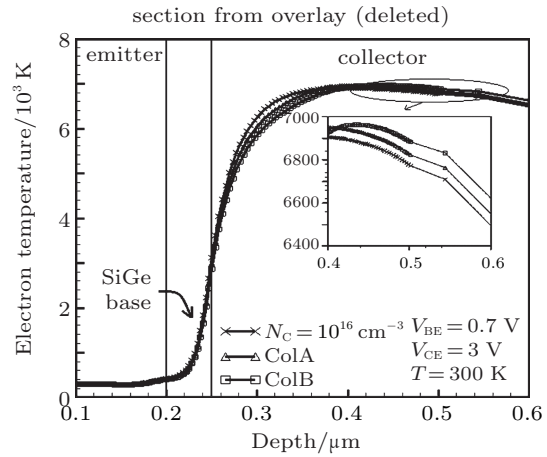


Fig. 11. Comparison of electron temperature for HBTs with a standard ($N_C = 1 \times 10^{16}$ cm^{-3}) collector doping, ColA, and ColB.

In addition, compared with the standard collector doping, the peak f_T with ColB is decreased by 0.8 GHz, caused by the composite of P^+ and N^- layers inside the CB SCR, which introduces some net charge into the CB depletion region, leading to widened CB SCR and increased τ_{CSCL},[16] and the peak f_T with ColA is decreased by 0.3 GHz, caused by the P^+ layer inside the CB SCR, which introduces more net charge into the CB depletion region. However, slight degradation occurs at a higher current and is often ignored in many circuit applications. Furthermore, the product of $f_T \times BV_{CEO}$ with ColB is the largest; it is improved from the 309.51 GHz·V of the standard collector doping to 326.35 GHz·V.

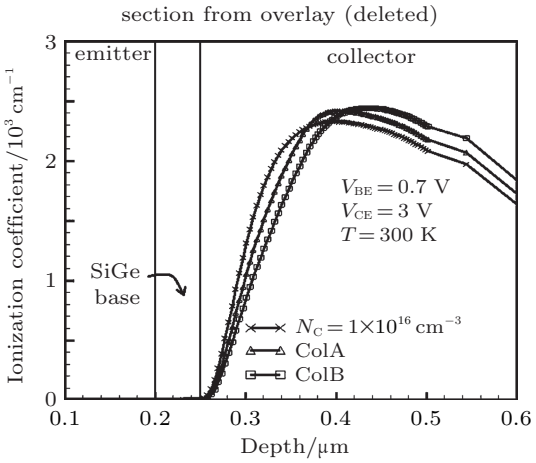


Fig. 12. Comparison of ionization coefficient for HBTs with a standard ($N_C = 1 \times 10^{16}$ cm^{-3}) collector doping, ColA, and ColB.

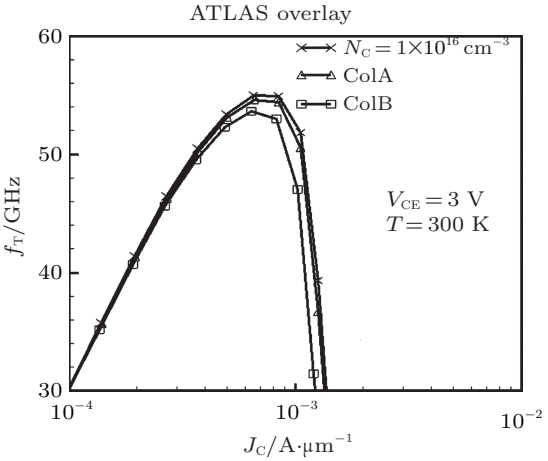


Fig. 13. Comparison of f_T versus J_C for HBTs with a standard ($N_C = 1 \times 10^{16}$ cm^{-3}) collector doping, ColA, and ColB.

4. Conclusion

Compared with the single decreasing collector doping, which is often used in the standard SiGe HBT, a novel collector doping is presented to improve the well-known tradeoff between the breakdown voltage and the cut-off frequency in the SiGe HBT. A composite of P^+ and N^- doping layers inside the CB SCR decreases the electric field and lowers the electron temperature near the CB metallurgical junction, consequently suppressing the impact ionization. As a result, compared with the standard collector doping, BV_{CEO} is improved and the product of $f_T \times BV_{CEO}$ is increased.

References

[1] Yuan J H and Cressler J D 2011 *IEEE Trans. Electron. Device* **58** 1655
[2] Jagannathan B, Khater M, Pagette F, Rieh J S, Angell D, Chen J, Florkey F, Golan D R, Greenberg R, Groves, Jeng S J, Johnson J, Mengistu E, Schonenberg K T, Schnalbel C M, Smith P, Stricker A, Ahlgren D, Freeman G, Stein K and Subbanna S 2002 *IEEE Trans. Electron. Device* **23** 258

[3] Zhang W R, Yang J W, Liu H J, He Y, Gao F Y and Liu L M 2004 *International Conference on Microwave and Milli-wave Technology (ICMMR/T)*, August 18–21, 2004 Beijing, China, p. 594
[4] Nellis K and Zampardi J 2004 *IEEE Journal of Solid-State Circuit* **39** 1746
[5] Rieh J S, Khater M, Freeman G and Ahlgren D 2006 *IEEE Trans. Electron. Device* **53** 2407
[6] Rieh J S, jagannathan B, Greenberg D, Freeman G and Subbanna S 2004 *Solid State Electronics* **48** 339
[7] Geynet B, Chevalier P, Brossard F, Vandelle B, Schwartzmann T, Buczko M, Avenier G, Dutartre D, Dambrine G, Danneville F and Chantre A 2009 *Solid State Electronics* **53** 873
[8] Xiong X Y, Zhang W, Xu J, Liu Z H, Chen C C, Huang W T, Li X Y, Zhong T and Qian P X 2004 *J. Semiconduct.* **25** 1238
[9] Donkers J J T M, Vanhoucke T, Agarwal P, Jueting R J E, Meunier B P, Vijayaraghavan M N, Magnee P H C, Verheijen M A, De K R and Slotboom J W 2004 *IEDM Technical Digest*, December 13–15, 2004 San Francisco, USA, p. 243
[10] Xue C L, Shi W H, Cheng B W, Yao F and Wang Q M 2007 *J. Semiconduct.* **28**(SUPPL) 435
[11] Zappa F, Lovati P and Lacaita A 1996 *IEEE IPRM*, April 21–25, 1996 Schwabisch Gmund, Germany, p. 628
[12] Xu X B, Zhang H M, Hu H Y and Li S C 2011 *Chin. Phys. B* **20** 108502
[13] Guo L L Feng Q, Hao Y and Yang Y 2007 *Acta Phys. Sin.* **56** 2895 (in Chinese)
[14] Li Q, Zhu J L, Wang W D and Wei X M 2011 *Chin. Phys. B* **20** 117202
[15] Song Q W, Zhang Y M, Zhang Q and Lü H L 2010 *Chin. Phys. B* **19** 087202
[16] Lü Y J, Xu D G, Liu P X, Lü D, Yao J Q, Wen Q Y and Zhang H W 2011 *Chin. Phys. B* **20** 104205